

Combined MEK and JAK/STAT3 pathway inhibition effectively decreases SHH medulloblastoma tumor progression

Jamie Zagozewski*¹, Stephanie Borlase*¹, Brent J. Guppy¹, Ludivine Coudière-Morrison¹, Ghazaleh M. Shahriary¹, Victor Gordon¹, Lisa Liang¹, Stephen Cheng¹, Christopher J. Porter, Rhonda Kelley, Cynthia Hawkins^{4,5}, Jennifer A. Chan^{6,7}, Yan Liang⁸, Jingjing Gong⁸, Carolina Nör⁹, Olivier Saulnier⁹, Robert J. Wechsler-Reya¹⁰, Vijay Ramaswamy^{4,9,11,12} & Tamra E. Werbowetski-Ogilvie^{1,13}

1 Department of Biochemistry and Medical Genetics, Rady Faculty of Health Sciences, University of Manitoba, Winnipeg, MB, Canada. 2 Ottawa Bioinformatics Core Facility, Ottawa Hospital Research Institute, Ottawa, ON, Canada. 3 Central Animal Care Services, University of Manitoba, Winnipeg, MB, Canada. 4 The Arthur and Sonia Labatt Brain Tumour Research Centre, The Hospital for Sick Children, Toronto, ON, Canada. 5 Department of Laboratory Medicine and Pathobiology, University of Toronto, Toronto, ON, Canada. 6 Department of Pathology & Laboratory Medicine, University of Calgary, Calgary, AB, Canada. 7 Arnie Charbonneau Cancer Institute, University of Calgary, Calgary, AB, Canada. 8 Pathology Department, NanoString Inc, Seattle, WA, USA. 9 Developmental and Stem Cell Biology Program, The Hospital for Sick Children, Toronto, ON, Canada. 10 Sanford Burnham Prebys Medical Discovery Institute, La Jolla, CA, USA. 11 Division of Haematology/Oncology, The Hospital for Sick Children, Toronto, ON, Canada. 12 Department of Medical Biophysics, University of Toronto, Toronto, ON, Canada. 13 CancerCare Manitoba Research Institute, Winnipeg, MB, Canada. *These authors contributed equally: Jamie Zagozewski, Stephanie Borlase

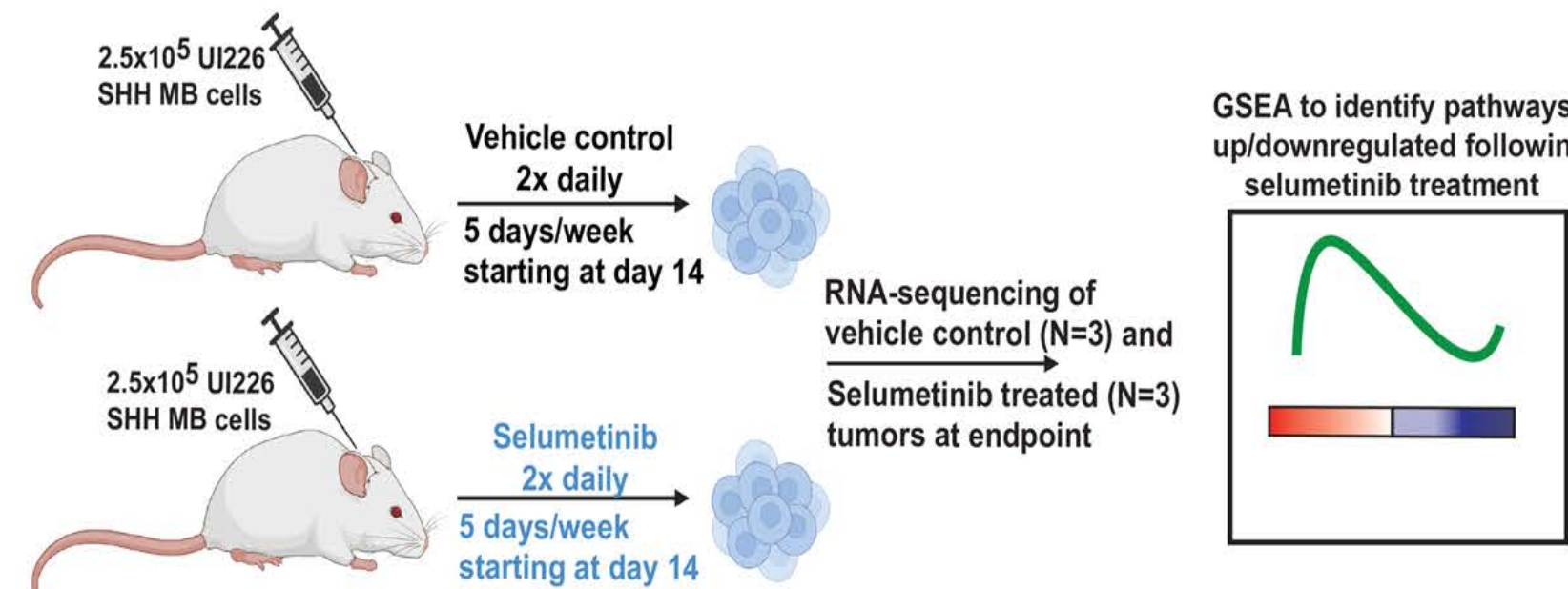
INTRODUCTION

- Medulloblastoma (MB) is the most common malignant pediatric brain tumor.
- MB is classified into 4 distinct molecular subgroups (WNT, SHH, Group 3, and Group 4) based on genomic alterations, gene expression profile, response to treatment and cell of origin.
- SHH MB is associated with an intermediate prognosis and characterized by dysregulations in the SHH signalling pathway.
- Due to the extensive heterogeneity between and within the subgroups, there is a critical need for subgroup-specific, functionally validated biomarkers and therapeutic strategies
- We previously identified CD271 as a diagnostic and prognostic marker in SHH MB, with CD271+ cells exhibiting elevated levels of MAPK signaling.
- Targeting the MAPK pathway with the MEK inhibitor selumetinib attenuated SHH MB tumor progression; however animals eventually succumbed to disease progression.

Hypothesis: We hypothesize that compensatory pathways play a role in SHH MB tumor progression and targeting these additional pathways will aid in enhancing survival.

METHOD

- RNA sequencing was performed on selumetinib vs. control treated UI226 SHH MB xenografts to evaluate the molecular mechanisms underlying selumetinib resistance in SHH MB xenografts.



- Tumorsphere assay and 3D collagen migration assay were performed following treatment with control, selumetinib, pacritinib (or AZD1480) or selumetinib+pacritinib (or AZD1480) to evaluate sphere formation and migration respectively *in vitro*
- In vivo* orthotopic xenograft mouse models were utilized to evaluate the effects of selumetinib, pacritinib or selumetinib+pacritinib vs. vehicle control on SHH MB.
- Multiplex digital spatial profiling was performed to explore the molecular changes following drug treatment in SHH MB xenografts

RESULTS

JAK/STAT3 pathway activity is upregulated following MEK inhibition *in vivo*

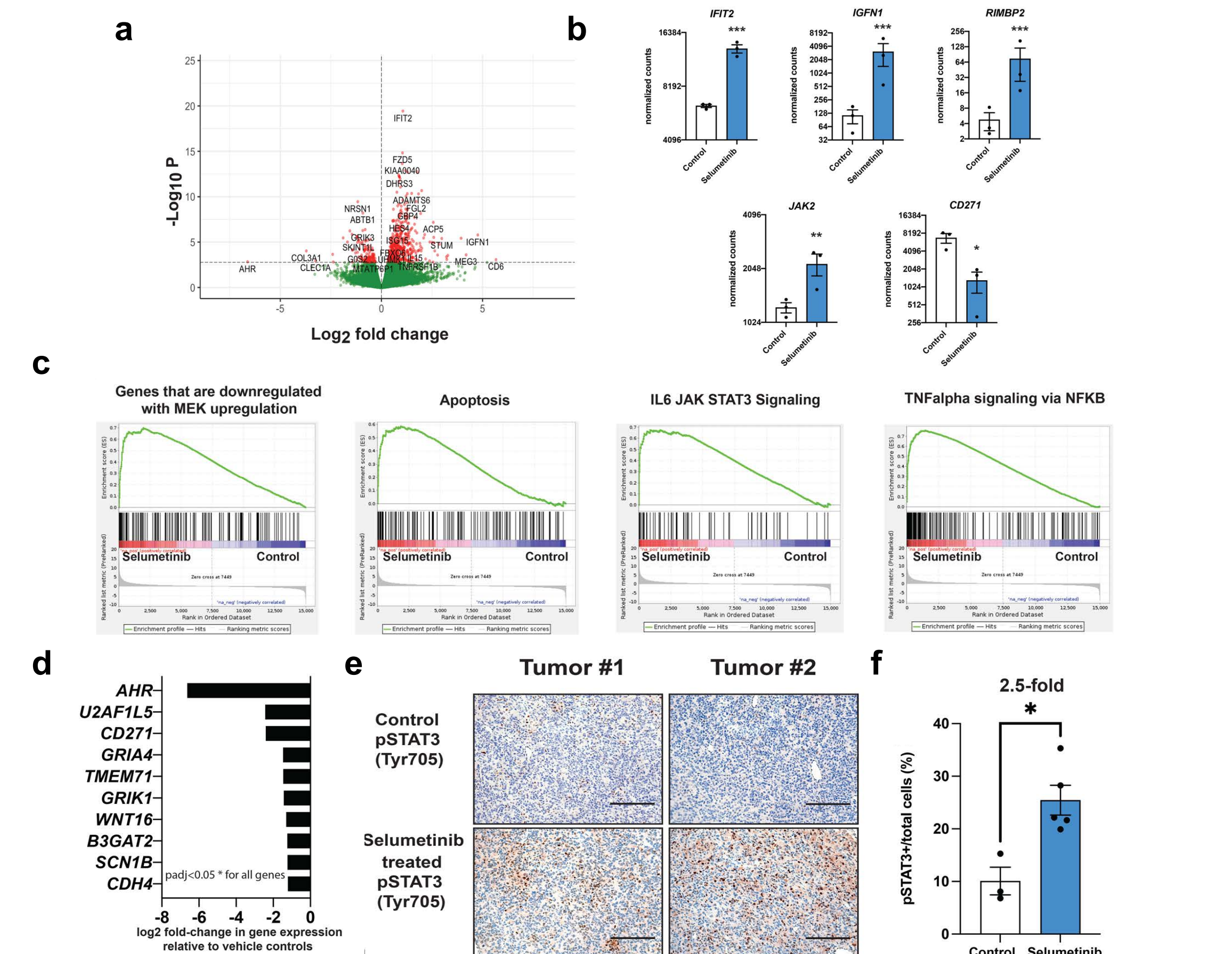


Figure 1. RNA sequencing of SHH MB xenografts from selumetinib vs. vehicle control treatment reveals upregulation of the JAK/STAT3 pathway. **a.** Volcano plot depicting the log2 fold change and p-values in RNA-seq data with points in red identifying the 576 significantly differentially expressed genes (FDR < 0.05). **b.** Normalized counts for representative differentially expressed transcripts from RNA-seq data. IFIT2, IGFN1, RIMBP2 and JAK2 are increased while CD271 expression is decreased in selumetinib-treated UI226 SHH MB xenografts relative to vehicle controls. $p < 0.05^*$, $p < 0.01^{**}$, $p < 0.001^{***}$. **c.** GSEA demonstrating that genes associated with a downregulated MEK signature, increased JAK/STAT3, TNFAlpha, and apoptosis signaling are enriched in genes sets that are upregulated in selumetinib-treated xenografts. $\text{padj} < 0.05^*$ for all signatures. **d.** Most significantly downregulated genes in selumetinib-treated xenografts. $\text{padj} < 0.05^*$ for all genes. **e.** Representative images of IHC staining for pSTAT3 (Tyr705) in FFPE sections from two independent control (upper) and selumetinib-treated (lower) UI226 SHH MB xenografts. Scale bar: 150 μm . **f.** Quantitative analyses of IHC pSTAT3 (Tyr705) staining in vehicle control (white) and selumetinib-treated (blue) xenografts. $P < 0.05^*$.

The JAK/STAT3 signalling signature is lower in SHH MB primary patient tumors

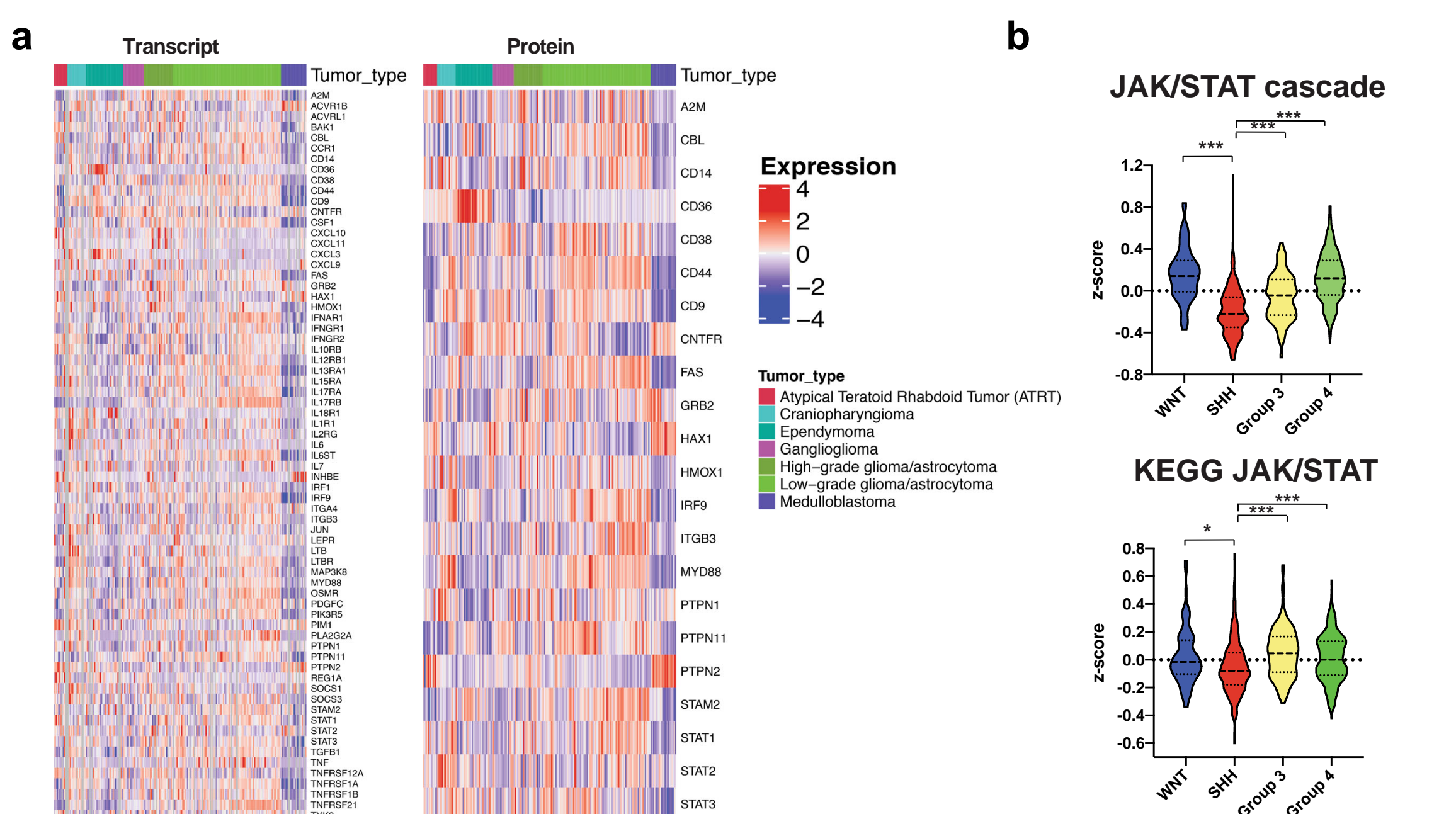


Figure 2. The JAK/STAT3 signalling signature is lower in SHH MB primary patient tumors. **a.** Heatmap illustrating transcript (left) and protein (right) levels of JAK/STAT3 signalling signature across 218 samples representing several classes of childhood brain cancer. Individual samples are aligned vertically into columns, with the 22 MB samples colored in purple. **b.** Violin plots depicting z-scores for 2 JAK/STAT signaling cascade transcriptome signatures across the 4 MB subgroups. Significance was determined by ANOVA, with a Tukey's test for multiple comparisons. $p < 0.05^*$, $p < 0.001^{***}$. For all violin plots, the center line is the median, the 25th and 75th percentiles are depicted by the lower and upper dotted lines, respectively and the extremes of the distribution extend to the minima and maxima.

Dual MEK + JAK/STAT3 pathway inhibition elicits a reduction in SHH MB tumorigenic properties *in vitro*

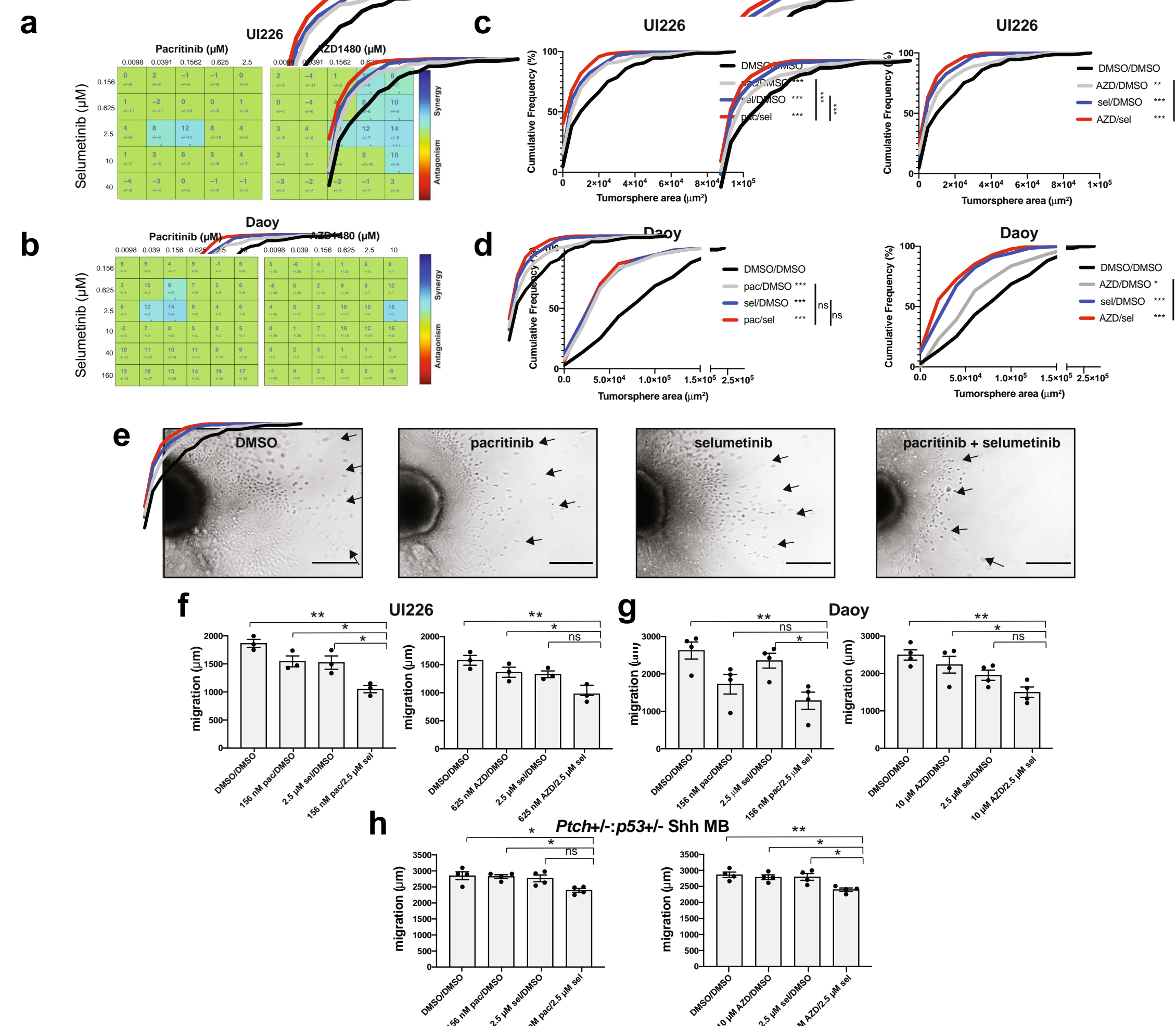


Figure 3. Dual MEK+JAK/STAT3 pathway inhibition elicits a reduction in SHH MB tumorigenic properties *in vitro*. **a-b.** Combeneffit synergy plots for UI226 (a) and Daoy (b) tumorspheres for pacritinib + selumetinib and AZD1480 + selumetinib. Numbers in the synergy matrices represent the percentage in tumorsphere size reduction that is greater than predicted by an additive model \pm SD. Drug combinations are color-coded as Blue: Synergy, Green: Additive, and Red: Antagonism. **c-d.** Cumulative frequency distribution of tumorsphere size for UI226 (c) and Daoy (d) following treatment with pacritinib + selumetinib or AZD1480 + selumetinib. Tumorsphere size was analyzed using two-sample Kolmogorov-Smirnov tests. $p < 0.05^*$, $p < 0.01^{**}$, $p < 0.001^{***}$. **e.** Representative images of migration through collagen type I gels following pacritinib, selumetinib or pacritinib + selumetinib treatment over 3 days. Scale bar: 400 μm . **f-h.** Quantification of cell migration in UI226 (f), Daoy (g) and Ptc1h+/-p53+/- SHH MB (h) aggregates following treatment with pacritinib + selumetinib or AZD1480 + selumetinib treatment. Error bars: SE. Results were analyzed using ANOVA followed by a Tukey's test for multiple comparisons. $p < 0.05^*$, $p < 0.01^{**}$.

Dual MEK + JAK/STAT3 pathway inhibition significantly improves survival and reduces tumor growth *in vivo*

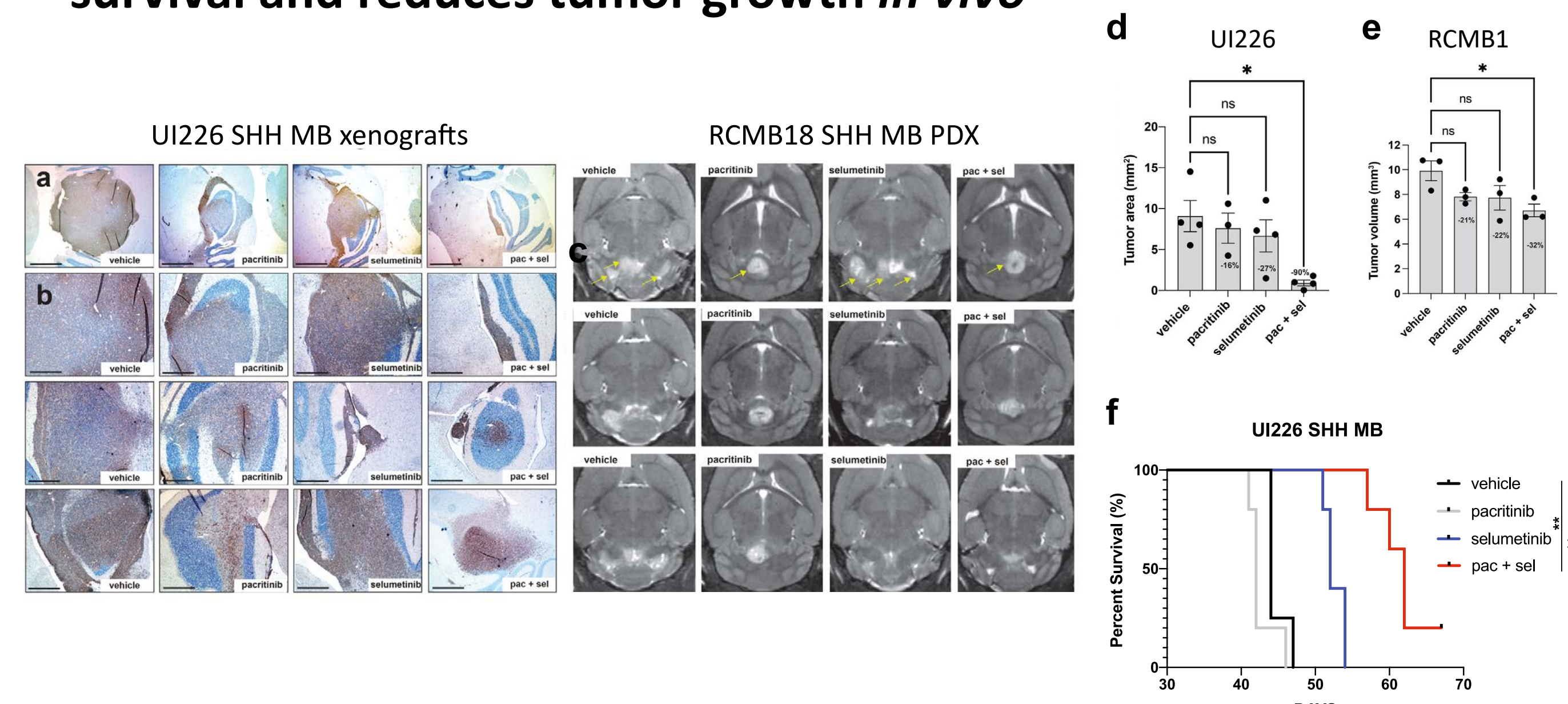


Figure 4. Dual MEK+JAK/STAT3 pathway inhibition significantly improves survival and decreases tumor growth *in vivo*. **a-b.** Representative IHC images of STEM121 levels at low magnification (a) and higher magnification (b) from three independent tumors from each of the vehicle control, pacritinib, selumetinib, and combination pacritinib + selumetinib treatment groups. Scale bars: 1500 μm (a) and 600 μm (b). **c.** Representative MRI images from three independent RCMB18 tumors representing the vehicle control, pacritinib, selumetinib, and combination pacritinib + selumetinib treatment groups. Arrows denote individual or multiple tumor lobes in representative images from the control group. **d-e.** ImageJ quantification of UI226 tumor area from STEM121 stained slides (d) and RCMB18 tumor volume from compiled MRI images (e) representing the vehicle control, pacritinib, selumetinib, and combination pacritinib + selumetinib treatment groups. Results were analyzed using ANOVA and a Dunnett's test for multiple comparisons. Error bars: SEM. $p < 0.05^*$. **f.** Kaplan-Meier curves following transplantation of NOD SCID mice with 2.5×10^5 UI226 SHH MB cells and treated with vehicle control, pacritinib, selumetinib, or pacritinib + selumetinib. P-value determined using the log-rank method. $p < 0.01^{**}$. Treatment was initiated 14 days following UI226 tumor cell injection.

Multiplex digital spatial profiling of proteins in drug-treated xenografts reveals shifted molecular dependencies

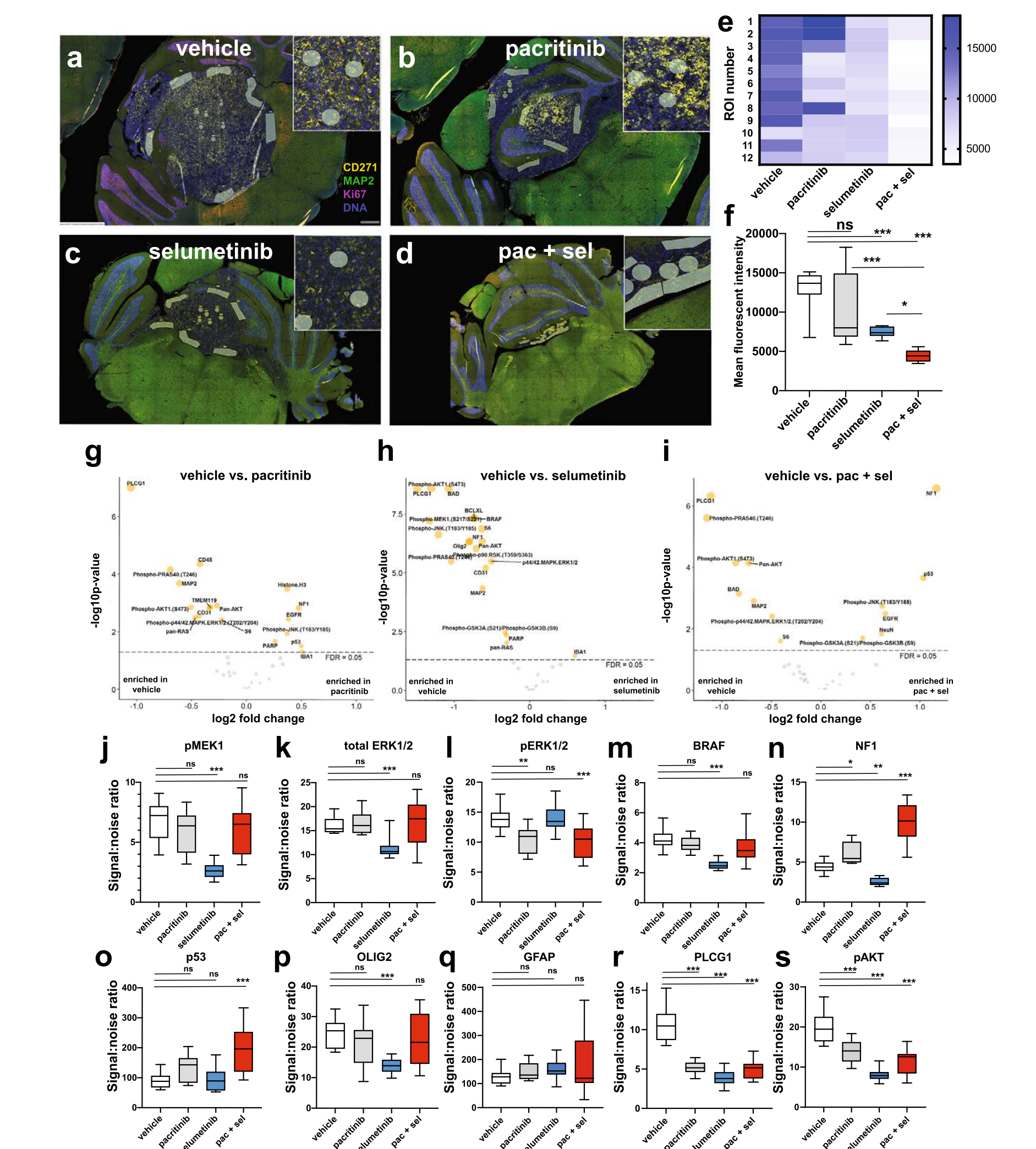


Figure 5. Multiplex digital spatial profiling of 56 proteins on MEK and/or JAK/STAT3 inhibitor-treated UI226 tumors *in vivo*. **a-d.** Representative immunofluorescent images depicting 12 regions of interests (ROIs) from the vehicle control (a), pacritinib (b), selumetinib (c) and pacritinib + selumetinib (d) treated samples utilized for analyses of 56 different proteins. Samples were stained for CD271 (yellow), MAP2 (green), Ki67 (pink), and Syto13 (blue) for tumor visualization. **e.** Heat map depicting CD271 levels across 12 ROIs in vehicle control, pacritinib, selumetinib, and pacritinib + selumetinib treated samples. **f.** Boxplots depicting quantification of CD271 levels by mean fluorescent intensity across vehicle control, pacritinib, selumetinib and pacritinib + selumetinib treated samples. Bars represent minimum and maximum counts. Significance was determined using ANOVA and a Tukey's test for multiple comparisons. $p < 0.05^*$, $p < 0.001^{***}$. **g-l.** Volcano plots displaying significantly differentially expressed proteins (based on signal-to-noise-ratio for each target relative to negative control IgG probes comparing the vehicle control to the pacritinib (g), selumetinib (h), and pacritinib + selumetinib-treated (i) tumor. For each volcano plot, significance of a specific protein was determined using a two-tailed t-test. FDR: false discovery rate. Of note, 36 of the 56 proteins reached threshold levels based on signal-to-noise ratio and were used for further analyses. **j-s.** Boxplots depicting select differentially expressed proteins based on signal-to-noise-ratio in vehicle control, pacritinib, selumetinib, and pacritinib + selumetinib treated samples. Bars represent minimum and maximum counts. ns: not significant. Significance was determined using ANOVA and a Dunnett's test for multiple comparisons. $p < 0.05^*$, $p < 0.01^{**}$, $p < 0.001^{***}$.

CONCLUSION

- Our study revealed that the JAK/STAT3 pathway exhibits increased activation in response to selumetinib treatment.
- We have shown that the combined inhibition of MEK and JAK/STAT3 pathway activity abrogates tumor properties in 3 different MB cell models *in vitro* as well as in *in vivo* models of SHH MB.
- Our study reveals new insight into the altered molecular mechanisms associated with selumetinib treatment and warrants further investigation into dual MEK and JAK/STAT3 inhibition as a novel combinatory therapeutic strategy for SHH MB.

